Identifying anomalous diffusion and melting in dusty plasmas

Yan Feng,* J. Goree, and Bin Liu
Department of Physics and Astronomy, The University of Iowa, Iowa City, Iowa 52242, USA
(Received 3 June 2010; revised manuscript received 2 August 2010; published 9 September 2010)

Anomalous diffusion in liquids and the solid-liquid phase transition (melting) are studied in two-dimensional Yukawa systems. The self-intermediate scattering function (self-ISF), calculated from simulation data, exhibits a temporal decay, or relaxation, with a characteristic relaxation time. This decay is found to be useful for distinguishing normal and anomalous diffusion in a liquid, and for identifying the solid-liquid phase transition. For liquids, a scaling of the relaxation time with length scale is found. For the solid-liquid phase transition, the shape of the self-ISF curve is found to be a sensitive indicator of phase. Friction has a significant effect on the timing of relaxation, but not the melting point.

DOI: 10.1103/PhysRevE.82.036403 PACS number(s): 52.27.Lw, 52.27.Gr, 61.20.Lc, 64.70.D−

I. INTRODUCTION

Dusty plasma is partially ionized gas containing micron-sized particles of solid matter [1]. In a plasma [1], the sheath above a lower electrode has electric fields that can levitate and confine highly charged particles, so that they are suspended. When only a single layer is suspended, the interaction between dust particles is a repulsive Yukawa potential [2]. Video microscopy allows imaging this two-dimensional (2D) suspension at an atomistic scale, so that we can track particles and measure their individual positions and velocities in each video frame, yielding the same kind of data as the molecular dynamics (MD) simulations, reported here.

Particles self-organize in a crystal-like triangular lattice with hexagonal symmetry due to strong interparticle interaction. In this strongly coupled plasma, the Coulomb interaction with nearest neighbors is so strong that particles do not easily move past one another [3]. In many experiments, the particles occupy only a single horizontal layer, and are often described as 2D experiments [1,4–8]. Dusty plasma is a driven-dissipative system [1], and its kinetic energy is determined by the balance of the energy input and dissipation. As the driven energy input increases, the lattice becomes disordered in a solid-liquid phase transition [1,8–13].

Random particle motion in dusty plasmas can be divided into several stages. Ballistic motion [14] occurs on a short time scale $<\omega_{pd}^{-1}$, while caging oscillations [15] happen on a typical time scale of $10\omega_{pd}^{-1}$. Here ω_{pd} is the nominal plasma frequency [16]. At later times, particles can escape their cages and diffuse. A current research topic that has not been resolved is whether this long-time random motion exhibits normal diffusion or anomalous diffusion. Experiments [14,17] and simulations [18–20] with these 2D systems have indicated superdiffusion, where the mean-square-displacement (MSD) increases with the time more rapidly than linear scaling, but other simulations suggest that random motion may be normal diffusion at sufficiently long times [21]. Identifications of normal diffusion and anomalous diffusion (e.g., superdiffusion here) have typically made use of dynamical measures: MSD time series, the probability distribution function (PDF) for particle displacements, and the velocity autocorrelation function (VACF) [18–21].

Data analysis methods used to study the solid-liquid phase transitions can be grouped in two categories, static and dynamic. Here, we term a method static if the input data can be a single snapshot of particle positions, but dynamic if it requires a series of positions for each particle. According to this classification, most attempts to identify phase transitions in dusty plasma experiments and MD simulations have employed only static structural measures, such as Voronoi diagrams and correlation functions for particle positions and angular orientation [1,8–13,22]. Sheridan used a static method of applying the empirical Lindemann criterion [13,23]. A dynamical method of identifying melting has been developed theoretically, using empirical criteria based on the long-time and short-time self-diffusion coefficients [24,25]; this has been demonstrated to be useful for simulations of both 2D [25] and 3D [24] systems.

Here we carry out dynamical analysis using the intermediate scattering function to characterize random motion. We study two physical processes: anomalous diffusion in liquids and the solid-liquid phase transition.

In Sec. II, we will review the intermediate scattering function briefly. In Sec. III, we will introduce our two MD Yukawa simulation methods: Langevin and frictionless. They will model a 2D dusty plasma. In Sec. IV, we will present results for the two physical processes: normal and anomalous diffusion in liquids, and the melting phase transition.

II. SELF-INTERMEDIATE SCATTERING FUNCTION

The intermediate scattering function (ISF) [26], which has been used widely in other fields, is also called the density-density correlation function [27]. The ISF is defined in terms of the particle trajectories:

$$F(\mathbf{k},t) = \frac{1}{N}\sum_i \sum_j \langle \exp(-i\mathbf{k}\cdot[\mathbf{r}_i(t) - \mathbf{r}_j(0)])\rangle. \quad (1)$$

Here, $\mathbf{r}_i(t)$ is the trajectory of the ith particle in the system consisting of N particles. The Fourier transform variable $\mathbf{k}$ is usually called a wave number, although no waves are studied using this method. Equation (1) makes use of an ensemble

*yan-feng@uiowa.edu

average $\langle \cdots \rangle$, which in practice is done by averaging for various initial starting times in place of $t=0$.

Calculating the ISF directly from Eq. (1) is a dynamical analysis method because it requires as its input data a time series of positions for each particle. This is the method we will use, as has been done previously in experiments with granular materials [28,29] and in MD simulations [30–32] of systems other than dusty plasmas.

Besides starting from measurements of particle trajectories, other experimental methods of obtaining the ISF have been devised for colloids [33], supercooled liquids [34], and polymer nanocomposites [35]. In these experiments, the ISF was determined from data produced by dynamic light scattering [33], x-ray photon correlation spectroscopy [35,36], or neutron spin echo spectroscopy [34,37]. A comparable experiment with a dusty plasma was reported by Khodataev *et al.* [38], using photon correlation spectroscopy to yield a function of wave number and time.

It is useful to compare the ISF, which is a time series, with two related functions. First, the dynamic structure factor [37] is the Fourier transform of the ISF; it is defined as $S(\mathbf{k},\omega)=\int_{-\infty}^{\infty}F(\mathbf{k},t)\exp(i\omega t)dt/2\pi$. This dynamic structure factor has been used for studying 2D Yukawa liquids in both theory [39] and simulations [40]. Second, phonon spectra, which are widely used for experimental and simulation data, have two parts, for longitudinal and transverse waves. The longitudinal phonon spectrum is related to the dynamic structure factor [41], although phonon spectra are more commonly computed differently, as a Fourier transform of the particle current [42].

The ISF is composed of two parts [37,43], $F(\mathbf{k},t)=F_s(\mathbf{k},t)+F_c(\mathbf{k},t)$. The most commonly used part is $F_s(\mathbf{k},t)$, which is often called the *incoherent* part, or the *self-ISF*:

$$F_s(\mathbf{k},t)=\frac{1}{N}\sum_i \langle \exp(-i\mathbf{k}\cdot[\mathbf{r}_i(t)-\mathbf{r}_i(0)])\rangle. \tag{2}$$

The less commonly used part is $F_c(\mathbf{k},t)$, which is called the *coherent* part,

$$F_c(\mathbf{k},t)=\frac{1}{N}\sum_{i\neq j}\sum_j \langle \exp(-i\mathbf{k}\cdot[\mathbf{r}_i(t)-\mathbf{r}_j(0)])\rangle. \tag{3}$$

The self-ISF, $F_s(\mathbf{k},t)$, is a measure of single-particle dynamics as a function of time. This makes it comparable to the MSD and PDF, which are also computed from the trajectories of individual particles recorded for a long time. Thus, the self-ISF can be used to study some of the same physical phenomena as MSD and PDF, such as random motion and the related idea of relaxation [29]. If random motion consists of normal diffusion, as for example with Brownian motion with a diffusion coefficient D, then [28,29,43]

$$F_s(\mathbf{k},t)\simeq \exp(-Dk^2t). \tag{4}$$

In Sec. IV A 2, we will generalize Eq. (4) for the case of anomalous diffusion, such as superdiffusion.

The self-ISF, Eq. (2), is often used by itself, without reporting the coherent part, Eq. (3). This is a common practice with particle trajectory data from experiments [28,29] and MD simulations [30–32] for various physical systems. Here, we will also use only the self-ISF for our Yukawa simulations of dusty plasmas.

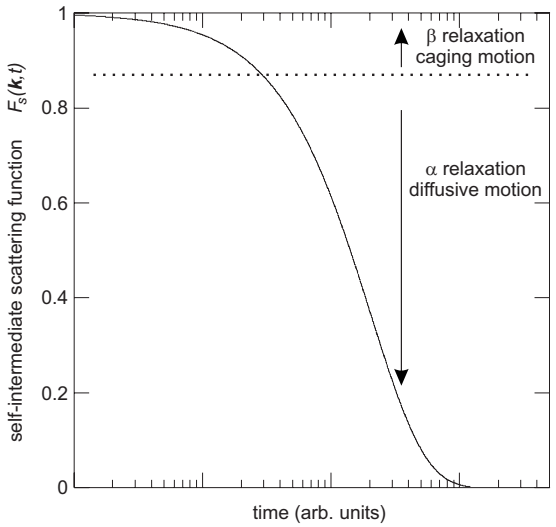

FIG. 1. A typical example of the self-intermediate scattering function (self-ISF) $F_s(\mathbf{k},t)$, sketched here to show how it begins at unity at $t=0$, and then relaxes gradually to zero as $t\to\infty$. Relaxation happens in two steps: early-time caging motion, and long-time diffusion. The self-ISF curve is often modeled by Eq. (5). The case shown here is for a normal liquid in 2D, and to reveal phenomena at a length scale corresponding to caging we chose $k=3.3a$, where a is the Wigner-Seitz radius, as defined in Sec. III.

A graph of the self-ISF typically reveals two stages of random motion. We illustrate this in Fig. 1 with a sketch of $F_s(\mathbf{k},t)$ for a normal liquid (not supercooled). The decay of the $F_s(\mathbf{k},t)$ curve is the signature of what is often called relaxation. Caging motion is indicated at short times. This early part of the curve is sometimes termed the fast β relaxation. Diffusion is indicated at long times, as particles gradually escape their cages [29]. In this later part of the curve, sometimes termed α relaxation, $F_s(\mathbf{k},t)$ gradually decays toward zero. Here, we will use the self-ISF two ways. We will inspect the shape of the self-ISF decay, and sometimes fit it to a stretched exponential [44]:

$$F_s(\mathbf{k},t)=\exp[-(t/\tau(k))^{\beta(k)}], \tag{5}$$

where $\tau(k)$ is a relaxation time. (Note that this use of the symbol β has no relation to the β relaxation.)

III. SIMULATION

A. Parameters

Equilibrium Yukawa systems are characterized by two dimensionless parameters: the coupling parameter Γ and the screening parameter κ [45,46]. Here, $\Gamma=Q^2/(4\pi\epsilon_0 ak_BT)$ and $\kappa\equiv a/\lambda_D$, where Q is the particle charge, T is the particle kinetic temperature, λ_D is the screening length, $a\equiv(n\pi)^{-1/2}$ is the Wigner-Seitz radius [16], and n is the areal number density. Another characteristic length is the lattice constant b for a defect-free crystal, which is $b=1.9046a$ for a 2D triangular lattice.

Our two simulation methods are the same in many respects. Both simulation methods use a binary interparticle interaction with a Yukawa pair potential,

$$\phi_{i,j} = Q^2(4\pi\epsilon_0 r_{i,j})^{-1}\exp(-r_{i,j}/\lambda_D), \tag{6}$$

where $r_{i,j}$ is the distance between the ith and jth particles. In both simulations, particles are only allowed to move in a single 2D plane. Conditions remained steady during each simulation run. For both simulations, the parameters we used were $N=16\,384$ particles in a rectangular box with periodic boundary conditions. The box had sides $128.3b \times 111.1b$. We truncated the Yukawa potential at radii beyond $12b$ [47]. The integration time step was $0.037\omega_{pd}^{-1}$, and simulation data were recorded for a time duration of $1777\omega_{pd}^{-1}$ in after the system reached its steady state. Other simulation details are presented in [18,47]. We report results with distances normalized by b, while time (and frictional damping rate ν) are normalized using the nominal plasma frequency $\omega_{pd} = (Q^2/2\pi\epsilon_0 ma^3)^{1/2}$ [16], where m is the particle mass.

We will next review the two simulation methods. They differ mainly in the equations of motion that are solved.

B. Langevin MD simulations

Our Langevin MD simulations take into account the dissipation due to frictional gas damping. The Langevin equations [18–21,47,48]. of motion for each particle is

$$m\ddot{\mathbf{r}}_i = -\nabla\sum \phi_{ij} - \nu m\dot{\mathbf{r}}_i + \zeta_i(t). \tag{7}$$

Trajectories $\mathbf{r}_i(t)$ are found by integrating Eq. (7) for all particles. Terms on the right-hand side include a frictional drag $\nu m\dot{\mathbf{r}}_i$ and a random force $\zeta_i(t)$. Note that we retain the inertial term on the left-hand-side in Eq. (7), unlike some Brownian-dynamics simulations of overdamped colloidal suspensions [49], where it is set to zero.

Our Langevin simulations mimic 2D dusty plasma experiments [1], but the driven-dissipation mechanism is only an approximation of the processes in experiments [47]. In our Langevin simulation, the heating and friction are explicitly coupled by the fluctuation-dissipation theorem [50,51]; this models collisions with gas atoms that provide both frictional drag and random kicks. However, besides random kicks from gas atoms, in dusty plasma there are some additional heating mechanisms arising from ion flow, particle charge fluctuations [52,53], and sometimes external laser manipulation [1,47] that are not explicitly modeled in our Langevin simulations.

C. Frictionless equilibrium MD simulations

In addition to our Langevin MD simulations which include friction, to obtain results in the frictionless limit, we also performed frictionless equilibrium MD simulations [18]. The equation of motion is

$$m\ddot{\mathbf{r}}_i = -\nabla\sum \phi_{ij}, \tag{8}$$

which we integrate for all particles. A Nosé-Hoover thermostat is applied to maintain a desired temperature [18].

This MD simulation method describes a frictionless atomic system. The particles collide among themselves, without any interaction with gas or other external influences. This method mimics thermal equilibrium conditions.

There are two parameters we can change in the frictionless MD simulations: Γ and κ. In the Langevin simulations, we can also vary ν. Varying Γ and κ is equivalent to varying temperature and density, and we will vary them over a range that allows us to simulate liquids or solids.

Our method is to generate trajectories $\mathbf{r}_i(t)$ for all particles by integrating Eqs. (7) or (8), and then to compute the self-ISF using Eq. (2). The self-ISF is a time series. We repeat its calculation for various wave numbers, k.

IV. RESULTS AND DISCUSSIONS

We present results for two physical processes for 2D systems under steady conditions. First, we evaluate whether random motion in a 2D liquid exhibits normal or anomalous diffusion. Second, we test whether the self-ISF can serve as a sensitive indicator of the phase transition between solid and liquid.

In this paper, relaxation refers to the decay of the self-ISF, $F_s(\mathbf{k},t)$, as shown in Fig. 1. The relaxation rate in general depends on the scale length, which is parameterized here by $1/k$. Using the terminology of other users of the self-ISF [29,54], the early stage of decay is termed β relaxation; during this early-time particles are mainly trapped within their cages formed by nearest neighbors. The later stage is termed α relaxation, and this corresponds to diffusion as particles decage. The term "decaging" refers to a particle's movement so that it is no longer trapped by the previous nearest neighbors. In a liquid, particles decage much more rapidly than in a solid, so that this β relaxation is much faster in liquids than solids.

A. Anomalous diffusion in 2D liquids

1. Results for the self-ISF

Results from our Langevin simulations are presented in Fig. 2 for typical liquid conditions far from the phase transition. Curves are shown as functions of time for various values of k. Note the smooth and gradual decay from unity to zero as time increases. This decay is the signature of relaxation. Here, the decay develops without any plateau. The lack of a plateau in the time-variation of the self-ISF is similar to what is seen in granular flows [28,29], but different from what is expected for supercooled liquids and glasses (cf. Fig. 3 of [54]).

To help quantify the relaxation that is observed in Fig. 2, we fit the time-dependence of the self-ISF to the empirical form Eq. (5). Since the relaxation process spans many decades of time, to perform this fit without biasing results toward long times, data points were sampled from the simulation results at time intervals equally spaced on a logarithmic scale. For a liquid far from the phase transition, Eq. (5) fits our simulation data points well (shown as solid lines in Fig. 2). The two free parameters for the fit, $\tau(k)$ and $\beta(k)$, help

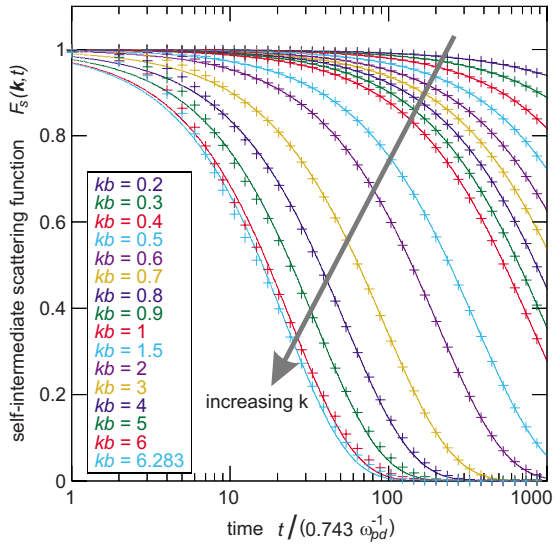

FIG. 2. (Color online) Time dependence of the self-ISF for various wave numbers (k) for the Langevin molecular dynamics (MD) simulation in the liquid regime: $\Gamma=200$, $\kappa=2$, and $\nu/\omega_{pd}=0.027$. The solid lines are the corresponding fits to Eq. (5). Quantities are normalized by parameters, such as the lattice constant b, as defined in Sec. III A.

quantify the relaxation process. We discuss their physical significance below.

2. Searching for anomalous diffusion

We develop two tools for identifying anomalous diffusion. Previous investigators have usually used the MSD, looking for a scaling with time that differs from the MSD $\propto t$ scaling expected for normal diffusion [14,17–19,21]. For 2D systems, data are typically fit to the form

$$\langle r^2(t)\rangle = 4Dt^{\alpha}, \tag{9}$$

where $\alpha=1$ is the case of normal diffusion, $\alpha>1$ is superdiffusion, and $\alpha<1$ is subdiffusion. (This use of the symbol α has no relation to the α relaxation mentioned above.) Here we introduce two other tools that are also based on how random motion develops with time: the scaling with τ vs. k, and the value of β. Recall that τ and β are the fitting parameters for Eq. (5).

Our first new tool is the power-law scaling of the fitting parameter τ as compared to k. To do this, we must first generalize Eq. (4) to allow for anomalous diffusion. Starting from Eq. (2), previous authors [43,55] have demonstrated that

$$F_s(\mathbf{k},t) \simeq \exp\left(-\frac{k^2\langle r^2(t)\rangle}{4}\right), \tag{10}$$

where we have substituted 4 in place of 6 in the denominator for two dimensions instead of three. Next, we substitute Eq. (9) in Eq. (10), yielding

$$F_s(\mathbf{k},t) \simeq \exp(-k^2Dt^{\alpha}) = \exp[-D(k^{2/\alpha}t)^{\alpha}]. \tag{11}$$

Examining the argument on the right-hand-side reveals the scaling

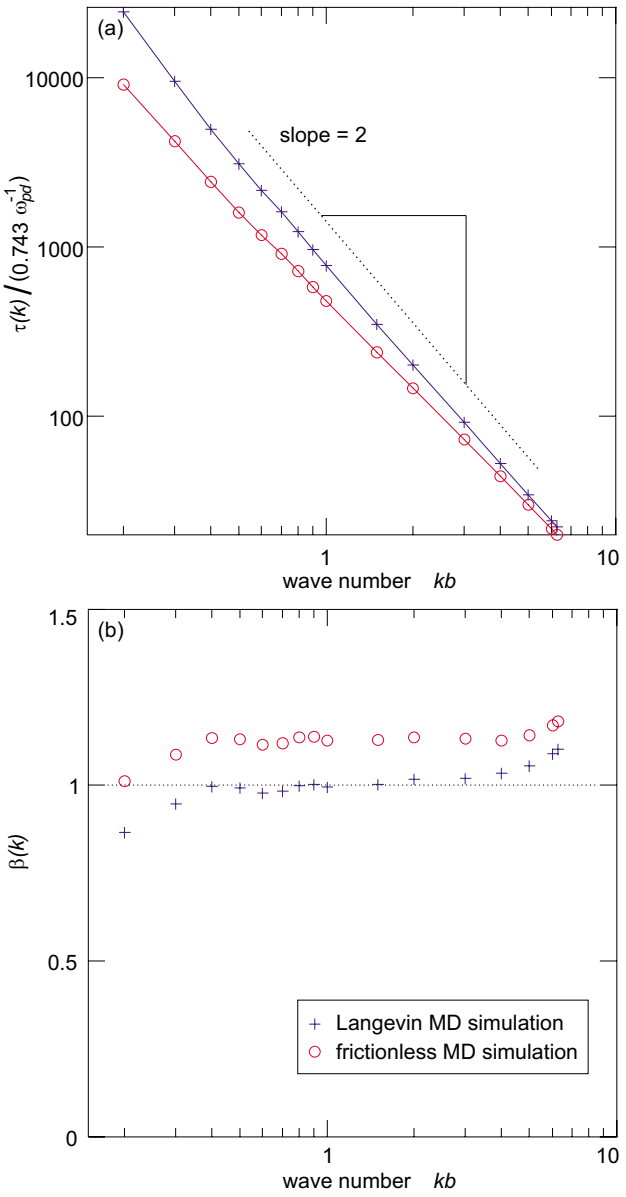

FIG. 3. (Color online) The fitting parameters, relaxation time τ in (a) and exponent β in (b), as a function of k. These cross symbols are from fitting the data in Fig. 2 for the Langevin MD simulation, and the circle symbols are for the frictionless MD simulation for the same liquid conditions, $\Gamma=200$, $\kappa=2$. We find that the scaling in (a) and the values of β in (b) are useful as indicators of anomalous diffusion.

$$\tau \propto k^{-2/\alpha}. \tag{12}$$

In the case of normal diffusion, $\alpha=1$, the scaling is $\tau\propto k^{-2}$, as previous authors have noted [28,29,43]. Here, we note that the superdiffusion case $\alpha>1$ has τ varying with a lesser power. Thus, the signature of superdiffusion will be a slope weaker than -2 when τ is plotted vs. k using log-log axes. Similarly, a slope stronger than -2 in the same $\tau-k$ plot is the signature of subdiffusion.

Our second new tool is the fitting parameter β for the self-ISF. Comparing Eqs. (5) and (11), we see that the value of β is essentially the same as α. The only difference is that

when using actual data, the value of β is generated by a fit, while α is generated by examining a log-log plot. The community of scientists who use the self-ISF traditionally uses β, although until now it has not been used as an indicator of superdiffusion. Scientists who use MSD to characterize superdiffusion, on the other hand, traditionally use α.

The two new diagnostic tools we described above may be useful for experiments in other fields where measurements allow one to obtain the self-ISF. While methods exist to distinguish anomalous diffusion from normal diffusion (using MSD, PDF, or VACF) if particle tracking is feasible, as in dusty plasma experiments [14] and MD simulations [18–21], other methods are needed when tracking is impossible. For example in a simple liquid, the motion of individual molecules cannot be tracked, but the self-ISF can be obtained using dynamic light scattering [43] or some other spectroscopic methods [34–37]. Thus, the two diagnostic tools presented above could find an application in such experiments.

3. Results for fitting the self-ISF

For the conditions of a liquid far from the phase transition, we use our two tools (scaling of τ vs k and the value of β) to test for anomalous diffusion. We use our two MD simulations, Langevin and frictionless. Ott and Bonitz [21] previously varied the values of friction ν and observation time over wide ranges, and using the MSD method prepared a diagram showing the conditions that favor normal diffusion or superdiffusion. This diagram, Fig. 3 of [21], predicts that the value of ν which we use in our Langevin simulation will yield normal diffusion, while the $\nu=0$ case of our frictionless simulation will yield superdiffusion over any reasonable observation time. Here we test whether our two cases, analyzed using our two new tools, yield the same conclusion as in [21].

For the τ vs k scaling, in Fig. 3(a) we find the scaling $\tau \propto k^{-2}$ for the Langevin MD simulations, and the scaling of $\tau \propto k^{-\gamma}(\gamma<2)$ for the frictionless MD simulations. In other words, random motion is diffusive for our frictional (Langevin) case, but superdiffusive for our frictionless case. This is in quantitative agreement with Fig. 3 of [21], prepared using MSD curves, which demonstrated that friction can inhibit superdiffusion [19,21].

For β, in Fig. 3(b) we find values near unity for our Langevin simulation, but a value definitely >1 for the frictionless simulation, for moderate values of k. This is again consistent with the conclusion of diffusive motion for our frictional (Langevin) case, but superdiffusive motion for the frictionless case. At extremely small or large values of k, however, β can be different. Figure 3(b) reveals an overall trend for β to increase with k, especially at extremely small or large values of k. Previous authors [28,29] have identified dynamic heterogeneities as the cause for $\beta<1$ for very small k, i.e., very large length scales. For large k, previous authors have not reported enhanced values of β like those we see in Fig. 3(b). One possible interpretation of our large k observation is that, at these short length scales, the self-ISF is affected more by caging motion than by random walks associated with decaging.

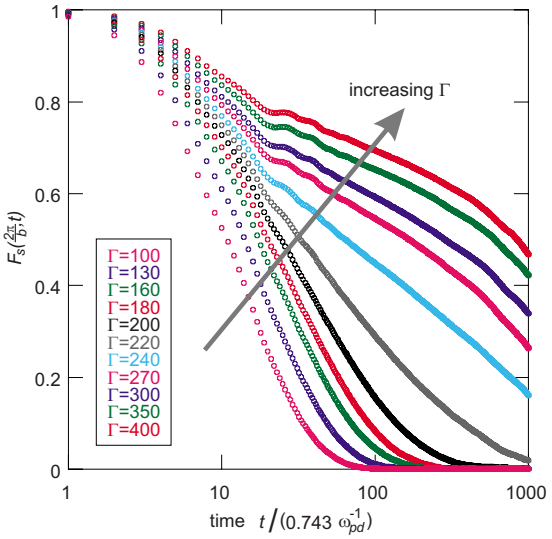

FIG. 4. (Color online) The self-ISF for the length scale corresponding to the lattice constant, $k=2\pi/b$. Results shown are for the Langevin MD simulations with constant values of $\kappa=1.2$ and $\nu/\omega_{pd}=0.027$. To search for an indication of a phase transition, Γ is varied over a range spanning both the solid and liquid phases. A phase transition near $\Gamma=200$ is indicated by a change in the curve's shape, and by larger gaps between curves for solids, $\Gamma>200$.

To summarize, we find that the relaxation of the self-ISF is a sensitive indicator to distinguish anomalous diffusion from normal diffusion. The indication can be made using either of the two fitting parameters, τ and β.

B. Solid-liquid phase transition

Simulation studies of the solid-liquid phase transition, which is also called an order-disorder transition or melting, are generally done using measures of static structural order, such as defects or correlation functions of particle position or bond orientation [1,8–13,22]. Dynamical measures can provide additional information that can be helpful for identifying a phase. Temperature is kind of dynamical measure for random motion, and so is the self-ISF.

Our first goal, for phase transitions, is to test the use of the self-ISF as an indicator of the phase transition. We perform tests that indicate that it is sensitive in distinguishing solids and liquids near the phase transition. This development is useful because the self-ISF is based on dynamics rather than structure. Our second goal is to determine what role friction plays in the phase transition. We will vary temperature and density, using the normalized quantities Γ and κ, and we will also vary the friction ν, to determine whether the self-ISF is sensitive to phases, and what role friction plays.

1. Dependence on Γ

We find that the self-ISF time series undergoes a sudden change at the melting point. This is seen for the self-ISF in Fig. 4 for our Langevin simulation. Here, we have chosen to present results for a small wave number $k=2\pi/b$, which is the wave number corresponding to a lattice constant so that the self-ISF indicates dynamics at the length scale of nearest

neighbors. As we varied Γ in Fig. 4, we held $\kappa=1.2$ and $\nu/\omega_{pd}=0.027$ as constants.

We note two features of the self-ISF curves in Fig. 4 that are different on either side of this sudden change. First, the gap between curves is much wider for low temperature (high Γ) conditions in the upper right of the figure as compared to the high temperature conditions in the lower left. We varied Γ in small steps near $\Gamma=200$, where we find the sudden change in the gaps between the self-ISF curves. Second, we identify different shapes for the decay of the self-ISF for low and high temperatures. For the high temperature (low Γ) conditions expected for liquids we found, in Sec. IV A, that the self-ISF decays according to the empirical law Eq. (5), but for low temperatures we found that Eq. (5) does not come even close to the shape of the curves in the upper right of Fig. 4.

Comparing to previous simulations that used structural measures, we can confirm that the sudden change in the self-ISF curve corresponds to the phase transition. Using a measure of local orientation order that exhibited a large jump at the phase transition, a phase transition curve for Γ vs. κ was reported, Fig. 6 in [22]. Interpolating their results, we find that the phase transition occurs at about $\Gamma=200$ for $\kappa=1.2$, for a 2D Yukawa system modeled with a frictionless MD simulation. This result is consistent with the sudden change that we observed in our self-ISF curves for $\kappa=1.2$ in Fig. 4: first, the curve's shape is changed; second, the curves are narrowly spaced for liquids ($\Gamma<200$) and widely spaced for solids ($\Gamma>200$). (One difference in the simulations of [22] and ours is our use of friction comparable to values in 2D dusty plasma experiments. We will explore the role of friction in Sec. IV B 4)

Thus, we conclude that the self-ISF curve is very sensitive to phase. It shows promise to become a reliable indicator of the phase transition, although further tests, for different physical parameters would be needed to confirm its reliability.

An attraction of this method is that the self-ISF is a dynamical rather than structural measure. Combining both dynamical and structural measures can be useful in distinguishing phases. For example, supercooled liquids have the structure of normal liquids, so that a dynamical measure is needed to distinguish the two. We note that other methods of using dynamical measures for such purposes include the Löwen criterion [24,25], which involves a comparison of diffusion coefficients computed in two limiting cases.

2. Dependence on κ

Varying only the density or κ, we again find the same two results as for varying Γ. There is a sudden change in the gaps between curves, and the curves take a different shape at a point that we can identify as the phase transition. This is seen in Fig. 5, where we changed κ in our Langevin simulations with $\Gamma=200$ and $\nu/\omega_{pd}=0.027$. The transition occurs at $\kappa=1.2$, which is consistent with Fig. 6 in [22].

3. Structure relaxation time

We investigate how rapidly disorder develops on the length scale of a cage, i.e., the interparticle spacing b. We will test whether it occurs with an Arrhenius or Vogel-Fulcher law as in other complex fluids such as colloids [56], granular materials [29], supercooled liquids and glasses [57]. We carry out this investigation by characterizing a decay time for the self-ISF. We could use the fit parameter $\tau(k)$ from Eq. (5), but for simplicity, rather than fitting the self-ISF, here we will adopt the practice of other authors of measuring the time required for the self-ISF to decay by a factor of $1/e$ [56,57]. This is done only for $k=2\pi/b$, corresponding to the length scale of a cage. Following the terminology used for example in the literature for colloids [56], supercooled liquids and glasses [57], this $1/e$ decay time, denoted here as $\tau_{2\pi/b}$, is called the "structure relaxation time." It is in principle the same as τ if $\beta=1$.

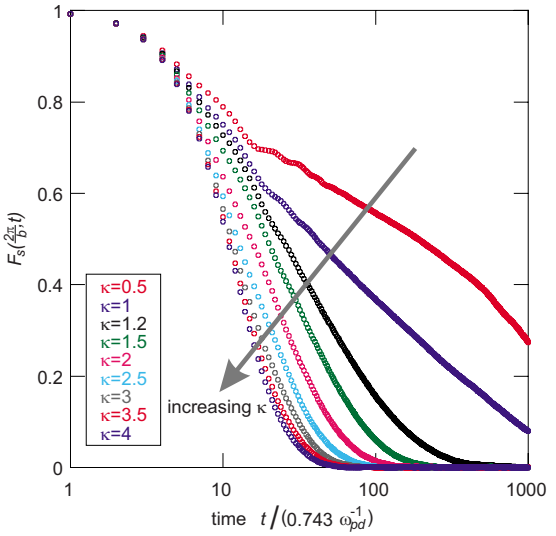

FIG. 5. (Color online) The self-ISF at $k=2\pi/b$, as in Fig. 4 but with varying κ. The simulations here are all Langevin MD simulations with constant values of $\Gamma=200$ and $\nu/\omega_{pd}=0.027$. To search for an indication of a phase transition, κ is varied over a range spanning both the solid and liquid phases. A phase transition near $\kappa=1.2$ is indicated by a change in the curve's shape, and the gaps between curves.

Results for the structure relaxation time $\tau_{2\pi/b}$ for the curves of Figs. 4 and 5 are shown in Fig. 6, revealing how $\tau_{2\pi/b}$ varies with temperature and number density. As the normalized temperature $1/\Gamma$ increases, the system melts and $\tau_{2\pi/b}$ decreases about one order of magnitude. The rate at which a structure relaxes, $1/\tau_{2\pi/b}$, increases with temperature, which is the same trend, for example, as for diffusion [58]. Melting also occurs as κ is increased. Plotting $\tau_{2\pi/b}$ vs. number density, in the inset of Fig. 6(b), we note a nearly linear scaling in the liquid regime.

The scaling we observe for $\tau_{2\pi/b}$ vs number density is different from the Arrhenius and Vogel-Fulcher laws. The Vogel-Fulcher law, which has been found empirically for other complex fluids [29,56,57], has $\tau_{2\pi/b}$ diverging to infinity as the number density increases toward the phase transition point. Here, $\tau_{2\pi/b}$ increases about an order of magnitude near the phase transition, but it does not diverge.

4. Dependence on ν

We find that friction can play an important role in the random motion of 2D Yukawa liquids, but only at large

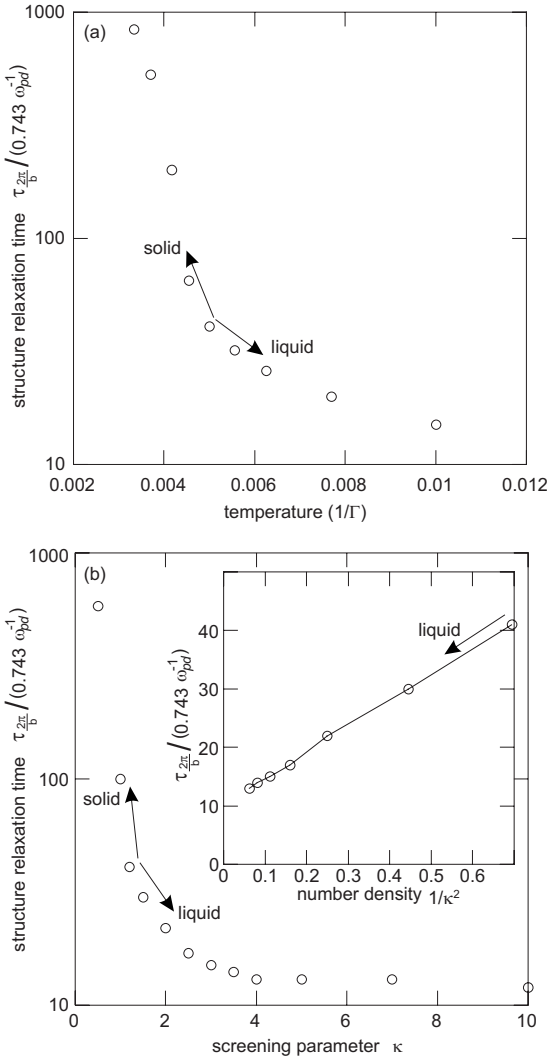

FIG. 6. Structure relaxation time measured from Figs. 4 and 5 as a function of (a) temperature and (b) screening parameter κ. The structure relaxation time in our 2D underdamped Yukawa system does not obey the Arrhenius law or Vogel-Fulcher law. The same data are plotted in the inset as a function of number density $1/\kappa^2$, for the liquid regime.

damping rates. This result is shown in Fig. 7 where we varied ν while holding Γ and κ constant in a liquid regime. We observe that the self-ISF curves all lie on top of one another for $\nu/\omega_{pd} \lesssim 0.03$, but not at higher damping rates where they decay more slowly as ν is increased. The curves at higher damping rates have the same general shape, but are retarded in time. In other words, friction has a significant effect on the timing of relaxation, but not the melting point. For the limiting case of no friction, we also include in Fig. 7 results for our frictionless equilibrium MD simulation, and these agree with the Langevin simulation for low friction $\nu/\omega_{pd} \lesssim 0.03$.

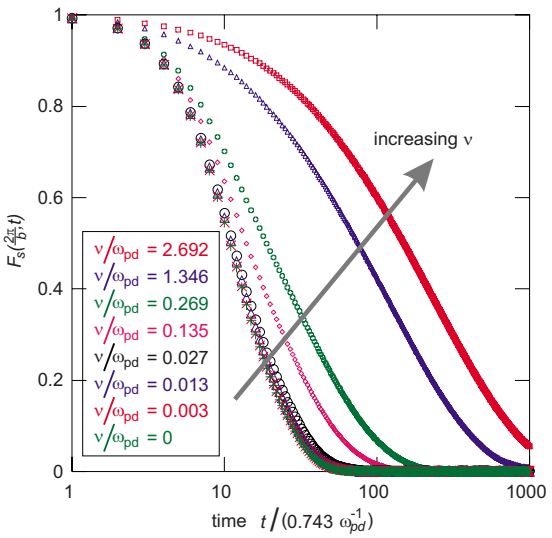

FIG. 7. (Color online) The role of friction in relaxation is investigated by computing the self-ISF at $k=2\pi/b$, for simulations of a liquid. The simulations here include both Langevin MD simulations and frictionless MD simulations in a liquid regime, with constant values of $\Gamma=200$ and $\kappa=3$. Unlike temperature and number density, changing the friction does not significant change the shape of the curves. The effect of friction in the self-ISF curves is a retardation of the decay at higher damping rate.

We note that Vaulina *et al.* [58] found that diffusion is mostly independent of damping rate, in the limit of low friction, which is similar to our results for relaxation.

We interpret the difference in the $F_s(2\pi/b,t)$ curves at various damping rates as indicating retardation of diffusion at high friction levels. At higher damping rate, the random motion of particles is resisted, then more energy is dissipated locally. As a result, the collective relaxation, which refers to the diffusion, will be retarded.

V. CONCLUSIONS

In conclusion, we have performed Yukawa MD simulations to study two physical processes in 2D dusty plasmas: anomalous diffusion in liquids and melting. For liquids, examining the decay or relaxation of the self-ISF reveals a scaling of the relaxation time vs length scale. This scaling is demonstrated to be useful for distinguishing normal and anomalous diffusion. The self-ISF is also demonstrated to be a sensitive indicator of the solid-liquid phase transition, i.e., melting. Friction has the effect of retarding relaxation.

ACKNOWLEDGMENTS

This work was supported by NSF and NASA.

[1] Y. Feng, J. Goree, and B. Liu, Phys. Rev. Lett. **100**, 205007 (2008).
[2] U. Konopka, G. E. Morfill, and L. Ratke, Phys. Rev. Lett. **84**, 891 (2000).
[3] S. Ichimaru, Rev. Mod. Phys. **54**, 1017 (1982).
[4] D. Samsonov, J. Goree, Z. W. Ma, A. Bhattacharjee, H. M. Thomas, and G. E. Morfill, Phys. Rev. Lett. **83**, 3649 (1999).
[5] A. V. Ivlev, U. Konopka, G. Morfill, and G. Joyce, Phys. Rev. E **68**, 026405 (2003).
[6] S. Nunomura, S. Zhdanov, D. Samsonov, and G. Morfill, Phys. Rev. Lett. **94**, 045001 (2005).
[7] S. Ratynskaia, K. Rypdal, C. Knapek, S. Khrapak, A. V. Milovanov, A. Ivlev, J. J. Rasmussen, and G. E. Morfill, Phys. Rev. Lett. **96**, 105010 (2006).
[8] V. Nosenko, J. Goree, and A. Piel, Phys. Plasmas **13**, 032106 (2006).
[9] H. M. Thomas and G. E. Morfill, Nature (London) **379**, 806 (1996).
[10] A. Melzer, A. Homann, and A. Piel, Phys. Rev. E **53**, 2757 (1996).
[11] R. A. Quinn and J. Goree, Phys. Rev. E **64**, 051404 (2001).
[12] C. A. Knapek, D. Samsonov, S. Zhdanov, U. Konopka, and G. E. Morfill, Phys. Rev. Lett. **98**, 015004 (2007).
[13] T. E. Sheridan, Phys. Plasmas **15**, 103702 (2008).
[14] B. Liu and J. Goree, Phys. Rev. Lett. **100**, 055003 (2008).
[15] C.-W. Io and L. I, Phys. Rev. E **80**, 036401 (2009).
[16] G. J. Kalman, P. Hartmann, Z. Donkó, and M. Rosenberg, Phys. Rev. Lett. **92**, 065001 (2004).
[17] B. Liu, J. Goree, and Y. Feng, Phys. Rev. E **78**, 046403 (2008).
[18] B. Liu and J. Goree, Phys. Rev. E **75**, 016405 (2007).
[19] L.-J. Hou, A. Piel, and P. K. Shukla, Phys. Rev. Lett. **102**, 085002 (2009).
[20] Z. Donkó, J. Goree, P. Hartmann, and B. Liu, Phys. Rev. E **79**, 026401 (2009).
[21] T. Ott and M. Bonitz, Phys. Rev. Lett. **103**, 195001 (2009).
[22] P. Hartmann, G. J. Kalman, Z. Donkó, and K. Kutasi, Phys. Rev. E **72**, 026409 (2005).
[23] F. A. Lindemann, Z. Phys. **11**, 609 (1910).
[24] H. Löwen, T. Palberg, and R. Simon, Phys. Rev. Lett. **70**, 1557 (1993).
[25] H. Löwen, Phys. Rev. E **53**, R29 (1996).
[26] P. N. Pusey, in *Liquids, Freezing and The Glass Transition*, edited by J. P. Hansen, D. Levesque, and J. Zinn-Justin (Elsevier, Amsterdam, 1991), Chap. 10.
[27] S. Kambayashi and Y. Hiwatari, J. Phys. Soc. Jpn. **56**, 2788 (1987).
[28] O. Dauchot, G. Marty, and G. Biroli, Phys. Rev. Lett. **95**, 265701 (2005).
[29] P. M. Reis, R. A. Ingale, and M. D. Shattuck, Phys. Rev. Lett. **98**, 188301 (2007).
[30] A. Meyer, Phys. Rev. B **81**, 012102 (2010).
[31] W. Kob and J.-L. Barrat, Phys. Rev. Lett. **78**, 4581 (1997).
[32] T. Abete, A. de Candia, E. Del Gado, A. Fierro, and A. Coniglio, Phys. Rev. Lett. **98**, 088301 (2007).
[33] W. van Megen and P. N. Pusey, Phys. Rev. A **43**, 5429 (1991).
[34] M. C. Bellissent-Funel, S. Longeville, J. M. Zanotti, and S. H. Chen, Phys. Rev. Lett. **85**, 3644 (2000).
[35] S. Srivastava, A. K. Kandar, J. K. Basu, M. K. Mukhopadhyay, L. B. Lurio, S. Narayanan, and S. K. Sinha, Phys. Rev. E **79**, 021408 (2009).
[36] X. Lu, S. G. J. Mochrie, S. Narayanan, A. R. Sandy, and M. Sprung, Phys. Rev. Lett. **100**, 045701 (2008).
[37] J. P. Hansen and I. R. McDonald, *The Theory of Simple Liquids*, 2nd ed. (Elsevier Academic Press, Amsterdam, 1986).
[38] Y. K. Khodataev, S. A. Khrapak, A. P. Nefedov, and O. F. Petrov, Phys. Rev. E **57**, 7086 (1998).
[39] M. S. Murillo and D. O. Gericke, J. Phys. A **36**, 6273 (2003).
[40] L.-J. Hou, Z. L. Mišković, K. Jiang, and Y.-N. Wang, Phys. Rev. Lett. **96**, 255005 (2006).
[41] Z. Donkó, G. J. Kalman, and P. Hartmann, J. Phys.: Condens. Matter **20**, 413101 (2008).
[42] B. Liu *et al.*, Phys. Plasmas **16**, 083703 (2009).
[43] W. van Megen, T. C. Mortensen, S. R. Williams, and J. Müller, Phys. Rev. E **58**, 6073 (1998).
[44] M. D. Ediger, C. A. Angell, and S. R. Nagel, J. Phys. Chem. **100**, 13200 (1996).
[45] H. Ohta and S. Hamaguchi, Phys. Plasmas **7**, 4506 (2000).
[46] K. Y. Sanbonmatsu and M. S. Murillo, Phys. Rev. Lett. **86**, 1215 (2001).
[47] Y. Feng, B. Liu, and J. Goree, Phys. Rev. E **78**, 026415 (2008).
[48] O. S. Vaulina, E. A. Lisin, A. V. Gavrikov, O. F. Petrov, and V. E. Fortov, Phys. Rev. Lett. **103**, 035003 (2009).
[49] H. Löwen, J. Phys.: Condens. Matter **4**, 10105 (1992).
[50] R. K. Pathria, *Statistical Mechanics* (Pergamon Press, Oxford, 1972).
[51] W. F. van Gunsteren and H. J. C. Berendsen, Mol. Phys. **45**, 637 (1982).
[52] R. A. Quinn and J. Goree, Phys. Rev. E **61**, 3033 (2000).
[53] G. Norman, V. Stegailov, and A. Timofeev, Contrib. Plasma Phys. **50**, 104 (2010).
[54] D. R. Reichman and P. Charbonneau, J. Stat. Mech.: Theory Exp. 2005, 05013.
[55] B. R. A. Nijboer and A. Rahman, Physica (Amsterdam) **32**, 415 (1966).
[56] R. Kurita and E. R. Weeks, e-print arXiv:0910.2628.
[57] T. Kawasaki, T. Araki, and H. Tanaka, Phys. Rev. Lett. **99**, 215701 (2007).
[58] O. Vaulina, S. Khrapak, and G. Morfill, Phys. Rev. E **66**, 016404 (2002).